Glasslike properties of a chain of particles with anharmonic and competing interactions

P. Reichert and R. Schilling
Institute of Physics, University of Basel, CH-4056 Basel, Switzerland
(Received 18 April 1985)

For a translationally invariant model of a chain of classical particles with anharmonic and competing nearest- and next-nearest-neighbor interactions, the existence of an infinite number of metastable chaotic equilibrium configurations is proved. Their pair distribution function exhibits more or less pronounced nearest-, next-nearest-, etc., neighbor peaks and the absence of long-range order (under certain conditions). The structure factor shows beside the usual peaks a sequence of extra peaks. The existence of two-level systems for such chaotic configurations is proved. Their energies and the barrier heights are calculated exactly. The corresponding density of states is not constant and shows a scaling property which leads to a power law $c(T)\sim T^{\tilde{d}}$ for the specific heat with a fractional exponent $\tilde{d}=\{\ln[p^2+(1-p)^2]\}/\ln|\eta|$, where $0<p<1$ characterizes the type of disorder and $\eta\gtrless 0$ depends only on the ratio of the nearest- and next-nearest-neighbor coupling constants. A pair potential is given for which these results remain true.

I. INTRODUCTION

It is a question of basic importance whether or not the rather irregular arrangement of atoms in an amorphous solid can be considered as a metastable equilibrium configuration obtained by the minimization of an interaction potential. To our knowledge there exist only numerical calculations, e.g., for the dense random packing of atoms[1] or for continuous random networks,[2] demonstrating this fact for a finite number of particles. But the question of whether in addition to the regular equilibrium configurations (crystalline and incommensurate) such irregular ones may also exist, in general, is still open from a *theoretical* point of view. This situation is comparable to the problem of the existence of turbulence. The intense studies of the *temporal chaotic* behavior of dynamical systems in the last few years[3] have led to a more microscopic understanding of turbulence and related phenomena and show the existence of irregular solutions of the corresponding equation of motion, e.g., irregular trajectories of particles. One of the characteristic features of temporal chaotic behavior is that there exist short-time but no long-time correlations. This is quite similar to amorphous solids which show short-range correlations between nearest-, next-nearest, and perhaps third-nearest neighbors but no long-range correlations in space. Therefore the following question arises: Can one find simple models for the interaction between particles which have metastable, spatially chaotic equilibrium configurations, and do these particles exhibit properties of amorphous solids?

What are typical properties of amorphous solids? Besides the characteristic behavior of the pair distribution function, reflecting the properties mentioned above, there exists a universal low-temperature behavior of, e.g., the specific heat $c(T)$ and the thermal conductivity $\kappa(T)$. This was first discovered experimentally by Zeller and Pohl[4] who had found that below 1 K $c(T)\sim T^n$ and $\kappa(T)\sim T^m$ with $n\approx 1$ and $m\approx 2$. Since the specific heat below 1 K exceeds that predicted by Debye's theory, there exist further low-energy excitations in addition to the phonons. A theoretical explanation was given independently by Anderson, Halperin, and Varma[5] and Phillips[6] by the postulation of tunneling modes or two-level systems. They argued that the corresponding density of states is constant on an energy scale below 1 K which implies a specific heat linear in T. Most experiments, however, show instead a power-law behavior with a broken exponent which may be larger than 1 ($<\approx 1.3$) (Ref. 7) or smaller than 1 ($>\approx 0.5$) (Ref. 8). These exponents depend on the material, the quenching rate, and the annealing temperature[9] as well as on the time scale of the measurements.[10] For a more comprehensive discussion of the low-temperature properties of amorphous solids we refer to Ref. 11.

Additional experimental evidence that the density of states $n(\epsilon)$ for the two-level systems is not constant was recently given by Molenkamp and Wiersma.[12] They deduced from photon-echo experiments on pentacene in polymethylmethacrylate that $n(\epsilon)\sim\epsilon^{0.3}$.

Up to now there exists little theoretical work which gives a microscopic justification of the tunneling model, and in all of this work models *without full translational invariance* are studied. For a one-dimensional Frenkel-Kontorova-like model Pietronero and Strässler[13] have calculated the energies and the density of states of the configurational excitations which represent two-level systems. Their numerical calculations for a system with 48 particles gave a density of states with gaps leading to a Schottky-like specific heat. Recently Geszti[14] used a nonideal Frenkel-Kontorova model with a mixture of springs of two different equilibrium lengths. He also obtained two-level systems (for the case where one type of the springs is dilute) but with $n(\epsilon)\sim\epsilon^{-1}$, which leads to a constant specific heat. The potential barriers, their correlations with the two-level systems, and the quantum corrections are not discussed in Refs. 13 and 14. Quite a

different approach to the two-level systems based on topological arguments is given by Rivier and Duffy.[15] But there the classical energies of all local minima are the same, and the two-level systems arise only because of the tunneling.

There exist of course many other characteristic properties of amorphous solids, such as localization of electrons due to the disorder leading to a special behavior of electrical conductivity, or the glass transition, etc. which will not be discussed here.

In the present paper we investigate the question: To what extent do systems with spatially chaotic equilibrium configurations exhibit pair distribution functions and structure factors resembling those of amorphous solids? We prove the existence of two-level systems and calculate their density of states, the potential barriers, and finally the low-temperature specific heat.

A partial answer with respect to the pair distribution function was found by the authors for a mathematical model[16] (referred to as I). There the Baker transformation, which is mixing, was used to construct one-dimensional chaotic configurations. Their pair distribution function $G(r)$ shows more or less pronounced nearest-, next-nearest-, etc., neighbor peaks and converges to 1 for $r\rightarrow\infty$, proving the lack of long-range order. Because the mixing behavior of the Baker transformation (or equivalently the Bernoulli shift) is the origin of the chaotic behavior of physical models [through its embedding (see I)], there was the hope to find similar results for $G(r)$ for physical models.

Recently we have presented a simple one-dimensional model for the interaction between particles for which this embedding of the Bernoulli shift and the existence of an infinite number of metastable and chaotic equilibrium configurations was shown analytically[17] (referred to as II). In particular we have shown in II that this model leads to a microscopic justification of the two-level systems (TLS) but with a density of states which is nonconstant. The corresponding low-temperature ($T<1$ K) specific heat exhibits a power-law behavior with a fractional exponent smaller than 1.

In this paper we give the details of the calculations of II, the geometric aspect of the embedding of the Bernoulli shift, a generalization of the model and the obtained results in II, as well as a discussion of $G(r)$. The organization of this paper is as follows: In Sec. II we present and motivate the model. The equilibrium configurations are derived in Sec. III, which also contains the details of the embedding. The pair distributions function $G(r)$ and the structure factor $S(k)$ are discussed in Sec. IV, and in Sec. V we obtain the energies of the TLS, the potential barriers, the density of states, and the specific heat. The generalization to a model with a pair potential and the discussion of our results are presented in Secs. VI and VII, respectively.

II. MODEL

In order to find a model with glasslike configurations we have restricted ourselves to one dimension. This of course makes the comparison with experiments difficult, but there may exist layered compounds or quasi-one-dimensional systems, e.g., polymer chains as those studied by Bonart,[18] for which the model we will discuss applies. But there is also quite a different reason why it is interesting to study one-dimensional models: The three-dimensional space cannot completely be tiled with regular tetrahedra (arising from the dense packing of hard spheres). This leads to geometrical competition or frustration which produces *topological defects*. Such topological defects play a crucial role for the existence and the physical properties of three-dimensional amorphous solids.[19] For one-dimensional systems *this* type of geometrical frustration and topological defects does *not* exist. Therefore it is also of interest to study amorphicity in one dimension.

The model we consider is an infinite chain of identical, classical particles each interacting up to its rth-nearest neighbors with potential energy:

$$V(\{u_n\})=\sum_n\sum_{l=1}^{r}V_l(u_{n+l}-u_n)\ , \tag{1}$$

where u_n is the position of the nth atom and V_l the interaction potential between the lth-nearest neighbors. The model (1) has two kinds of symmetry:

$$V(\{u_n+a\})=V(\{u_n\}),\ \text{for all } a\ , \tag{2a}$$

stating the translational invariance, and

$$V(\{u_{n+m}\})=V(\{u_n\}),\ \text{for all integers } m\ , \tag{2b}$$

which is the symmetry being left over from the original permutation invariance when the positions of the atoms are labeled by their order in the chain. The first one, (2a), allows to introduce the atomic distances

$$v_n=u_{n+1}-u_n\ , \tag{3}$$

and (2b) together with (2a) implies the existence of an invariant, which is the internal stress of the chain:

$$I(u_{n-r+1},u_{n-r+2},\ldots,u_{n+r})=\sum_{l=1}^{r}\sum_{j=1}^{l}V_l'(u_{n+j}-u_{n+j-l})\ . \tag{4}$$

$I(u_{n-r+1},u_{n-r+2},\ldots,u_{n+r})$ is independent of n along a stationary configuration, i.e., a solution of

$$\frac{\partial V}{\partial u_n}(u_{n-r},u_{n-r+1},\ldots,u_{n+r})=0\ . \tag{5}$$

This can be easily proven using (5). The existence of such an invariant was already discussed by Janssen and Tjon[20] for $r=3$. Equation (4) is the general form for arbitrary r.

One necessary condition for the existence of chaotic equilibrium configurations is the anharmonicity of at least one of the potentials V_l. This anharmonicity causes a nonlinearity in Eq. (5), which may lead to a class of chaotic solutions. A second characteristic property for systems with chaotic behavior is the existence of frustration effects which may be of geometrical, energetical, or of any other origin.

The simplest model which takes both conditions into account, where in particular the frustration is caused by

competing interactions, is a piecewise parabolic potential for V_1:

$$V_1(v)=\tfrac{1}{2}C_1\{[v-a_+-a_-\sigma(v)]^2 - [c-a_+-a_-\sigma(v)]^2\}\ ,\quad C_1>0\ , \tag{6a}$$

where $a_\pm=\frac{1}{2}(a_2\pm a_1)$, a_1, a_2 are the positions of the minima, c the location where both parabola are patched together, and

$$\sigma(v)=\mathrm{sgn}(v-c)\in\{-1,1\}\ , \tag{6b}$$

and a harmonic potential for V_2,

$$V_2(v)=\tfrac{1}{2}C_2(v-b)^2,\quad C_2\gtrless 0\ , \tag{6c}$$

where b is the corresponding equilibrium distance. Similar exactly solvable models have been used by Villain and Gordon[21] and Axel and Aubry[22] in order to describe spatially modulated phases. Figure 1 shows three typical situations for V_1 and V_2. The situation in Fig. 1(a), which contains as a special case the symmetric double-well potential studied in II, differs qualitatively from Figs. 1(b) and 1(c). If in Fig. 1(a) $C_2=0$ it is obvious that there exists an infinite number of chaotic equilibrium configurations which remain true if $C_2\neq 0$, but small enough. However, for Figs. 1(b) and 1(c) there exists only the crystalline configuration for $C_2=0$ while for $C_2\neq 0$, but not too large, chaotic equilibrium configurations may exist due to the competition between V_1 and V_2. In order for the anharmonicity to be relevant the nearest-neighbor distances have to be distributed around c, the location of the cusp in V_1. If the cusp is on the left (right) of the minimum, such that V_1 is repulsive (attractive) for $v\approx c$, V_2 has to be attractive (repulsive) at distances of the order of $2c$. (Figures 1(b) and 1(c) illustrate both situations.)

The case $C_1<0$ is excluded because all the chaotic equilibrium configurations are unstable in this case as will be discussed later.

Finally we mention that a situation like that in Fig. 1(a) could also model a system with two different types of (extented) particles of equilibrium size a_1 and a_2, respectively. V_1 would be associated with an internal (elastic) degree of freedom, and V_2 could describe the interaction between the particles.

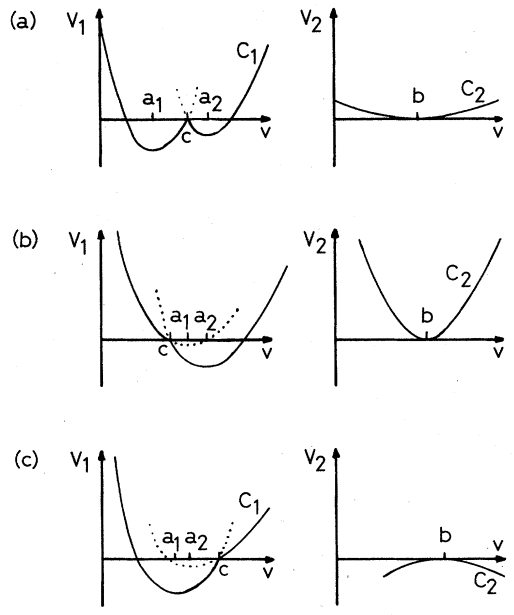

FIG. 1. Nearest- and next-nearest-neighbor potential (a) double-well-like potential; (b) and (c), single-well potential.

III. EQUILIBRIUM CONFIGURATIONS

A. Stationary solutions

Substituting (1) and (6) into (5) and assuming the internal stress I to be zero, we get for the equilibrium distances v_n the nonlinear difference equation:

$$2\gamma v_n+v_{n-1}+v_{n+1}=\phi(v_n)\ , \tag{7a}$$

with

$$\phi(v_n)=2[b+(\gamma-1)a_+]+2(\gamma-1)a_-\sigma(v_n)\ , \tag{7b}$$

$$\gamma=1+C_1/2C_2\ . \tag{7c}$$

Using the Green's function G of the difference operator [left-hand side (lhs) of (7a)], (7a) can be written as

$$v_n=\sum_m G(n-m)\phi(v_m)\ . \tag{8}$$

The Fourier transform $\tilde{G}(q)$ of the Green's function is easily obtained:

$$\tilde{G}(q)=[2(\gamma+\cos q)]^{-1}\ ,$$

from which one gets by contour integration

$$G(n)=\eta(1-\eta^2)^{-1}\eta^{|n|}\ , \tag{9a}$$

where

$$\eta=-\gamma[1-(1-\gamma^{-2})^{1/2}]\ . \tag{9b}$$

Using this and (7b) we get from (8):

$$v_n=A+\tfrac{1}{2}B\frac{1-\eta}{1+\eta}\left[\sigma(v_n)+\sum_{i=1}^{\infty}\eta^i[\sigma(v_{n-i})+\sigma(v_{n+i})]\right]\ , \tag{10a}$$

and with (9a):

$$v_n=A+\tfrac{1}{2}B\frac{1-\eta}{1+\eta}\left[\sigma_n+\sum_{i=1}^{\infty}\eta^i[\sigma(v_{n-i})+\sigma(v_{n+i})]\right]\ , \tag{10a'}$$

where

$$A=(1-\eta)^{-2}[(1+\eta)^2a_+-2\eta b]\ ,$$
$$B=2a_-(1-\eta)^{-2}(1+\eta)^2\ . \tag{10b}$$

Equation (10a) or (10a') represents a self-consistency equation for the stationary configuration $\{v_n\}$. If we replace $\{\sigma(v_n)\}$ on the right-hand side (rhs) by a given sequence $\sigma=\{\sigma_n\}$ of Ising variables $\sigma_n=\pm 1$, we obtain a configuration $\{v_n(\sigma)\}$ for any such sequence σ. This configuration $\{v_n(\sigma)\}$ is a solution of (10a) or (10a') if and only if

(i) v_n are positive and bounded, and (ii) if the self-consistency condition,

$$\sigma_n=\sigma[v_n(\{\sigma_i\})]\ , \tag{10c}$$

is fulfilled. It is obvious from (10a') that v_n is bounded for $|\eta|<1$. A necessary condition that (10c) holds is

$$v_n(\{\sigma_i\equiv -1\})<v_n(\{\sigma_i\equiv 1\}) \tag{11a}$$

for all n, which is true if

$$a_1<a_2\ . \tag{11b}$$

From (10a') we get

$$A-\frac{B}{2}\frac{(1-\eta)(1+|\eta|)}{(1+\eta)(1-|\eta|)}\le v_n\le A+\frac{B}{2}\frac{(1-\eta)(1+|\eta|)}{(1+\eta)(1-|\eta|)}\ . \tag{12}$$

Thus $v_n>0$ for all n if the (lhs) of (12) is positive, which is true if

$$b<\frac{(1+\eta)^2}{2\eta}a_1,\quad \text{for } 0<\eta<1 \tag{13a}$$

$$b>\frac{(1+\eta)^2}{2\eta}a_1+2a_+,\quad \text{for } -1<\eta<0\ . \tag{13b}$$

With use of (10a') again, (v_n-c) can be written as follows:

$$v_n-c=A+\tfrac{1}{2}B\frac{1-\eta}{1+\eta}\left[\sigma_n+\sum_{i\,(\neq 0)}\eta^{|i|}\sigma_{n-i}\right]-c\ . \tag{14}$$

A lower (upper) bound of (v_n-c) for $\sigma_n=+1(-1)$ is easily obtained from (14) such that the self-consistency is satisfied if

$$(v_n-c)_{\text{lower bound}}>0,\quad \text{for } \sigma_n=+1 \tag{15a}$$

$$(v_n-c)_{\text{upper bound}}<0,\quad \text{for } \sigma_n=-1 \tag{15b}$$

which leads with (11b), i.e., $a_->0$, to the condition:

$$-(1+|\eta|)(1-3|\eta|)a_-<(1-\eta)^2c+2\eta b$$
$$-(1+\eta)^2a_+<(1+|\eta|)(1-3|\eta|)a_-\ . \tag{16}$$

It is obvious that (16) can only be fulfilled if

$$|\eta|<\tfrac{1}{3}\ , \tag{17}$$

i.e., if $|\eta|<\frac{1}{3}$ there exists a range for (a_1,a_2,c,b) such that the conditions (13) and (16) hold for *all* sequences σ, and therefore $\{v_n(\sigma)\}$ is a stationary solution. It is easy to show that these solutions are uniquely determined by σ.

What we have found above has the following physical meaning: If $|\eta|<\frac{1}{3}$ and if (a_1,a_2,c,b) are in an appropriate range determined by (16), *an arbitrary* configuration $\{v_n'\}$ will relax to an equilibrium configuration $\{v_n(\sigma)\}$ for an interaction potential given by Eq. (6). The sequence σ is given by $\sigma_n=\sigma(v_n')$, i.e., the Ising variables σ_n do *not* change during the relaxation process.

B. Embedding of the Bernoulli shift

In this section we discuss the embedding of the Bernoulli shift which is characteristic for the chaotic behavior.[23] This will provide the connection to the mathematical model studied in I. The reader who is not interested in this aspect may skip this more technical exposition.

Denoting $v_{n-1}=x_n$ and $v_n=y_n$, the difference equation (7) can be written as a two-dimensional map

$$(x_{n+1},y_{n+1})=F(x_n,y_n)\ , \tag{18a}$$

where

$$F(x,y)=(y,\ -x-2\gamma y+\phi(y))\ , \tag{18b}$$

which represents a dynamical system with discrete time n. Consider the rhomb R bounded by the eigendirections of the fixed points (x_i^*,y_i^*), $i=1,2$ of F (see Fig. 2), which exist only if $a_1<a_2$ in agreement with (11b).

Because the Bernoulli shift has two fixed points, it is a necessary condition for the embedding that (x_i^*,y_i^*) exist. It is easy to show that all points outside R diverge under iteration of F or F^{-1}. It is obvious that the set of all bounded orbits is

$$C=\bigcap_{n=-\infty}^{\infty}F^n(R)\ . \tag{19}$$

Because F is piecewise linear, the structure of the set C can be derived exactly. The action of F in a neighborhood of R is analogous to a map containing a Smale horseshoe[24] if the points P_1 and P_2 (Fig. 2) lie outside R. The difference to the continuous case of Smale is that instead of folding R it is cut into two pieces which overlap with R (see Fig. 2). The image of each of these pieces is again cut into two pieces which overlap with $R\cap F(R)$, etc. Figure 3 illustrates this procedure and shows the sets

$$C_{n_0}=\bigcap_{n=-n_0}^{n_0}F^n(R)$$

for $n_0=1,2$ and $\eta>0$. The limit set $C=C_\infty$ is a Cantor set.[25] Such a Cantor set was already obtained by Aubry[26]

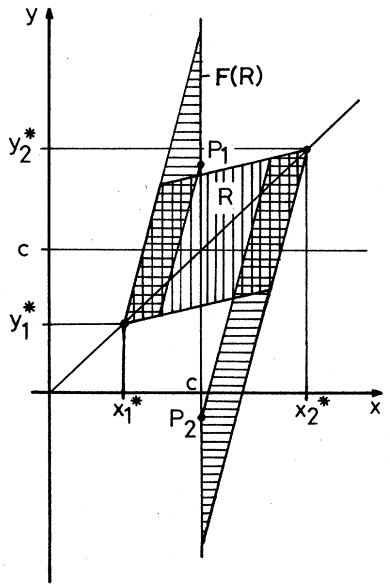

FIG. 2. Rhombus R (hatched vertically) and its image $F(R)$ (hatched horizontally) for $\eta>0$.

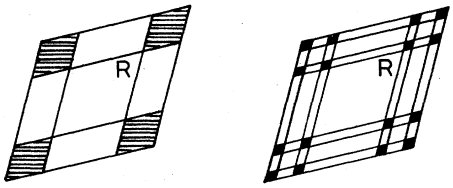

FIG. 3. C_{n_0} for $n_0=1$ (left) and $n_0=2$ (right).

for a two-dimensional map related to a Frenkel-Kontorova-type model.

The important requirement for the embedding of the Bernoulli shift is that P_1 and P_2 lie outside R which just happens if the inequality (16) is fulfilled. Thus the conditions (11b) and (16) for which the self-consistency is fulfilled also guarantee the embedding of the Bernoulli shift, which means that there exists a bijective map

$$\varphi:\ C\to M=\{-1,1\}^{\mathbb{Z}}$$

such that

$$F\mid_C=\varphi^{-1}\circ S\circ\varphi\ , \tag{20}$$

where $S: M\to M$ with

$$(S\sigma)_i=\sigma_{i+1} \tag{21}$$

is the Bernoulli shift. Using (18) and (21) it is easy to prove that (20) holds, if we choose

$$\varphi^{-1}(\sigma)=\left[A+\frac{B}{2}\frac{1-\eta}{1+\eta}\sum_i\eta^{|i|}\sigma_i,\ A+\frac{B}{2}\frac{1-\eta}{1+\eta}\times\sum_i\eta^{|i|}\sigma_{i+1}\right], \tag{22}$$

which follows from (10a'), but which can also be obtained by a geometric construction of the embedding.[27] The Cantor set C is given by

$$C=\varphi^{-1}(M)\ . \tag{23}$$

C. Energy of the equilibrium configurations

Substituting (10a) into (6a) and (6b) and using a sum rule for the Green's function, we get after simple but laborious calculations the energy $E(v(\sigma))$ of an equilibrium configuration $v(\sigma)$:

$$E(\sigma)\equiv E(v(\sigma))=e_0\sum_n 1-h\sum_n\sigma_n+\sum_{\substack{n,m\\ n\neq m}}J(n-m)\sigma_n\sigma_m\ , \tag{24a}$$

with

$$e_0=\frac{-C_1}{2}\left[\frac{1+\eta}{1-\eta}a_-^2+\frac{\eta}{(1-\eta)^2}b^2-\frac{4\eta}{(1-\eta)^2}ba_+ +c^2-2ca_++\left[\frac{1+\eta}{1-\eta}\right]^2a_+^2\right],$$

$$h=C_1(1-\eta)^{-2}a_-[(1+\eta)^2a_+-(1-\eta)^2c-2\eta b]\ , \tag{24b}$$

$$J(n)=J_0\eta^{|n|}\ ,$$

$$J_0=-\frac{C_1}{2}\frac{1+\eta}{1-\eta}a_-^2\ .$$

A similar Ising-like model with exponentially decaying coupling constant and external field was also obtained in Refs. 13, 14, 21, and 22 for the equilibrium configurations.

D. Metastability

In order to investigate the metastability of the equilibrium configurations (10) we have to determine the phonon frequencies ω which are related to the eigenvalues of the Jacobian $\partial^2V/\partial u_i\partial u_j$ at the considered stationary configuration. Using (1) and (6), we get

$$\frac{\partial^2V}{\partial u_i\partial u_j}=2(C_1+C_2)\delta_{i,j}-C_1(\delta_{i,j+1}+\delta_{i,j-1})-C_2(\delta_{i,j+2}+\delta_{i,j-2})\ , \tag{25}$$

which is *independent* of $\{u_n\}$. Therefore the eigenvalues can easily be calculated, and we find for the phonon frequencies

$$\omega(q)=\{2[C_1(1-\cos q)+C_2(1-\cos 2q)]/m\}^{1/2}\ , \tag{26}$$

where m is the mass of the particles. That it is possible to classify the frequencies by a wave number q, although we are considering disordered configurations, is due to the fact that for our model the Jacobian does not depend on the configuration. For

$$C_1>0,\quad C_2>-C_1/4\ , \tag{27}$$

which is equivalent to $|\eta|<1$, $\omega(q)$ is real for *all* stationary configurations and therefore all of them are metastable. The phonon frequency vanishes at $q=0$, which is just the Goldstone mode related to the translational symmetry (2a). Because the self-consistency condition requires $|\eta|<\frac{1}{3}$, the metastability is automatically guaranteed. For $C_1<0$ all the solutions are unstable.

E. Classification of the typical equilibrium configurations

The ground state of our model is always periodic (crystalline), either with period one or period two. This fact is generally true for a one-dimensional system with nearest- and next-nearest-neighbor interactions and does *not* depend on the special form of V_1 and V_2. For our case the period-one and period-two ground states are represented by $\sigma_n\equiv+1$, $\sigma_n\equiv-1$ and $\sigma_{2n}\equiv 1(-1)$, $\sigma_{2n+1}\equiv-1(+1)$, respectively. Which of these three types of crystalline

configurations is the ground state depends on (a_1, a_2, c, b) and $\mathrm{sgn}C_2$. We will not discuss the ground-state properties in more detail, because we are interested in the chaotic configurations. In the following we consider a special class of chaotic equilibrium configurations; that is, those configurations which correspond to random sequences σ of $+1$'s (probability p) and -1's (probability $1-p$). By random we mean that each possible finite subsequence of the doubly infinite sequence σ appears with probability $p^{n_1}(1-p)^{n_2}$ if n_1 and n_2 denote the number of $+1$ and -1, respectively, appearing in the subsequence. We call this class of sequences p-normal which is a straightforward generalization of the definition of normal numbers (see Niven[28]). In particular the p-normality implies that σ_n and σ_m, $n \neq m$, are uncorrelated.

If we use the symmetric or antisymmetric double-well-like potential [Fig. 1(a)] in order to model a system with two different types of extended components A_1 and A_2, a p-normal sequence represents a disordered, binary alloy $(A_1)_{1-p}(A_2)_p$. Note that in II we have discussed only the case $p=\frac{1}{2}$.

Besides this special class there also exist other chaotic configurations represented by sequences which are not p-normal. For instance one type is given by $\sigma_n=1$ for $n \neq km$ and σ_n random (± 1) for $n=mk$ for a fixed integer k and all integers m. But such a chaotic sequence represents a *microcrystalline* structure with grain size proportional to k. In the present paper we will not discuss either this special type of configurations or any other configurations belonging to a σ which is not p-normal. From these expositions it becomes clear that a sequence σ characterizes the type of *quenched bond disorder.*

Using (24) the energy $e(p)$ per atom for a p-normal σ can be calculated. We get

$$e(p)=e_0+(2p-1)h+(2p-1)^2\frac{2\eta}{1-\eta}J_0 \ . \tag{28}$$

Thus two configurations with different p_1 and p_2 differ by a macroscopic energy.

F. Influence of further anharmonicity

Let us add a potential $\bar{V}_1(x)$, which also contains terms of higher order than x^2, to the nearest-neighbor potential $V_1(x)$ [Eq. (6a)]. Then the rhs of the difference equation (7a) is replaced by

$$\bar{\phi}(\bar{v}_n)=\phi(\bar{v}_n)-C_2^{-1}\bar{V}_1'(\bar{v}_n) \ , \tag{29}$$

and Eq. (8) becomes

$$\bar{v}_n=\sum_m G(n-m)\bar{\phi}(\bar{v}_m) \ , \tag{30}$$

which can be solved by iteration. This we will demonstrate for

$$\bar{V}_1(x)=\frac{\bar{C}_1}{4}x^4 \ . \tag{31}$$

Then,

$$\bar{\phi}(\bar{v}_n)=\phi(\bar{v}_n)+\alpha\bar{v}_n^3 \ , \tag{32a}$$

where

$$\alpha=-\bar{C}_1/C_2 \ . \tag{32b}$$

If we put the ansatz

$$\bar{v}_n(\sigma,\alpha)=\sum_{\nu=0}^{\infty}\alpha^\nu v_n^{(\nu)}(\sigma) \tag{33}$$

into (30), and using (32), we get under the assumption that

$$\sigma(v_n)=\sigma(\bar{v}_n) \tag{34}$$

[v_n is given by (10a)]:

$$\begin{aligned} &v_n^{(0)}(\sigma)=v_n(\sigma) \ , \\ &v_n^{(\nu)}(\sigma)=\sum_m G(n-m)\sum_{\substack{\nu_1,\nu_2,\nu_3 \\ \nu_1+\nu_2+\nu_3=\nu-1}} v_m^{(\nu_1)}(\sigma)v_m^{(\nu_2)}(\sigma)v_m^{(\nu_3)}(\sigma) \ , \\ &\nu \geq 1 \ . \end{aligned} \tag{35}$$

The solution of the recursion relation (35) can be written as follows:

$$\begin{aligned} v_n^{(\nu)}(\sigma)=A^{(\nu)}&+\sum_{\mu=1}^{\nu}B_\mu^{(\nu)}\sum_m\sum_{i_1,i_2,\ldots,i_\mu}G(n-m)\prod_{\lambda=1}^{\mu}G(i_\lambda)\sigma_{n-i_1-i_2-\cdots-i_\mu} \\ &+\sum_{\mu_1,\mu_2}B_{\mu_1\mu_2}^{(\nu)}\sum_m\sum_{\substack{i_1,i_2,\ldots,i_{\mu_1}, \\ j_1,j_2,\ldots,j_{\mu_2}}}G(n-m)\prod_{\lambda=1}^{\mu_1}G(i_\lambda)\prod_{\lambda=1}^{\mu_2}G(j_\lambda)\sigma_{n-i_1-i_2-\cdots-i_{\mu_1}}\sigma_{n-j_1-j_2-\cdots-j_{\mu_2}}+\cdots \ , \end{aligned} \tag{36}$$

where the coefficients $A^{(\nu)}$, $B_\mu^{(\nu)}$, $B_{\mu_1\mu_2}^{(\nu)}$, etc. are functions of (a_1,a_2,c,b) and η.

We have estimated $|v_n^{(\nu)}(\sigma)|$ and we have found that there exists α_0 such that the power series (33) converges for $\alpha<\alpha_0$. Because of the continuity of $\bar{v}_n(\sigma,\alpha)$ for $\alpha<\alpha_0$ and because $\min_n|v_n-c|$ is finite for $|\eta|<\frac{1}{3}$, the self-consistency condition (34) is fulfilled for α small enough. Therefore the power series (33) represents a solution of the generalized model, and the embedding of the Bernoulli shift remains true.

If $V_2(x)$ would become anharmonic then the corresponding two-dimensional map $F(x,y)$ gets non-area-preserving which could lead to quite a different chaotic behavior, that is, a behavior on a strange attractor (see Ref. 3). But this will not be discussed in the present paper.

IV. PAIR DISTRIBUTION FUNCTION AND STRUCTURE FACTOR

In this section we discuss the distribution function $G_j(r)$ of the jth-nearest-neighbor distances, the pair distribution function $G(r)$, and its Fourier transform $S(k)$ at $T=0$ K for the chaotic equilibrium configurations of Sec. III, thus generalizing the results of I. All the figures in this section are obtained for the following values of the parameters: $a_1=3.0$ Å, $a_2=3.5$ Å, $c=3.9$ Å, $b=5.6$ Å, and $\eta=0.2$ for which (11b), (13), and (16) are fulfilled.

A. Distribution of jth-nearest-neighbor distances

For j small $G_j(r)$ can be determined explicitly using (10a') and assuming σ to be p-normal. In particular we obtain $G_1(r)$ as follows: The probabilities for a nearest-neighbor distance $v_n(\sigma)$ with $\sigma_n=+1$ and $\sigma_n=-1$ are p and $1-p$, respectively. From (10a') we easily obtain the bounds of the corresponding intervals $\hat{I}_{+1}$ and $\hat{I}_{-1}$ which have the property that

$$v_n\in\hat{I}_{+1}=\left[A+\frac{B}{2}\frac{1-\eta}{1+\eta}\frac{1-3|\eta|}{1-|\eta|},\ A+\frac{B}{2}\frac{1-\eta}{1+\eta}\frac{1+|\eta|}{1-|\eta|}\right],\ \text{with probability } p$$
$$v_n\in\hat{I}_{-1}=\left[A-\frac{B}{2}\frac{1-\eta}{1+\eta}\frac{1+|\eta|}{1-|\eta|},\ A-\frac{B}{2}\frac{1-\eta}{1+\eta}\frac{1-3|\eta|}{1-|\eta|}\right],\ \text{with probability } 1-p\ . \tag{37}$$

From (37) the significance of $|\eta|<\frac{1}{3}$ becomes again obvious, namely for $|\eta|<\frac{1}{3}$ both domains for v_n do not overlap (Fig. 4). Increasing the resolution one step more, each of the intervals $\hat{I}_+$ and $\hat{I}_-$ decomposes into three disjoint (for $|\eta|<\frac{1}{3}$) subintervals, etc.

In general for a resolution of order $B\eta^\nu$ the νth order distribution function $G_1^{(\nu)}(r)$, which is normalized to $A+(p-\frac{1}{2})B$, the mean lattice constant, is analytically given by

$$G_1^{(\nu)}(r)=\left[\tfrac{1}{2}+(p-\tfrac{1}{2})\mu_0\right](1-p)^{2(\nu-1-\mu-\mu')}[2p(1-p)]^{\mu}p^{2\mu'}\frac{1+\eta}{1-\eta}\frac{1-|\eta|}{2|\eta|^{\nu}}\frac{A+(p-\frac{1}{2})B}{B}\ , \tag{38a}$$

for

$$r\in\hat{I}_{\mu_0,\mu_1,\ldots,\mu_{\nu-1}}=\left[A+B\frac{1-\eta}{1+\eta}\left[\sum_{i=0}^{\nu-1}|\eta|^i\mu_i-\hat{\delta}_\nu\right],\ A+B\frac{1-\eta}{1+\eta}\left[\sum_{i=0}^{\nu-1}|\eta|^i\mu_i+\hat{\delta}_\nu\right]\right], \tag{38b}$$

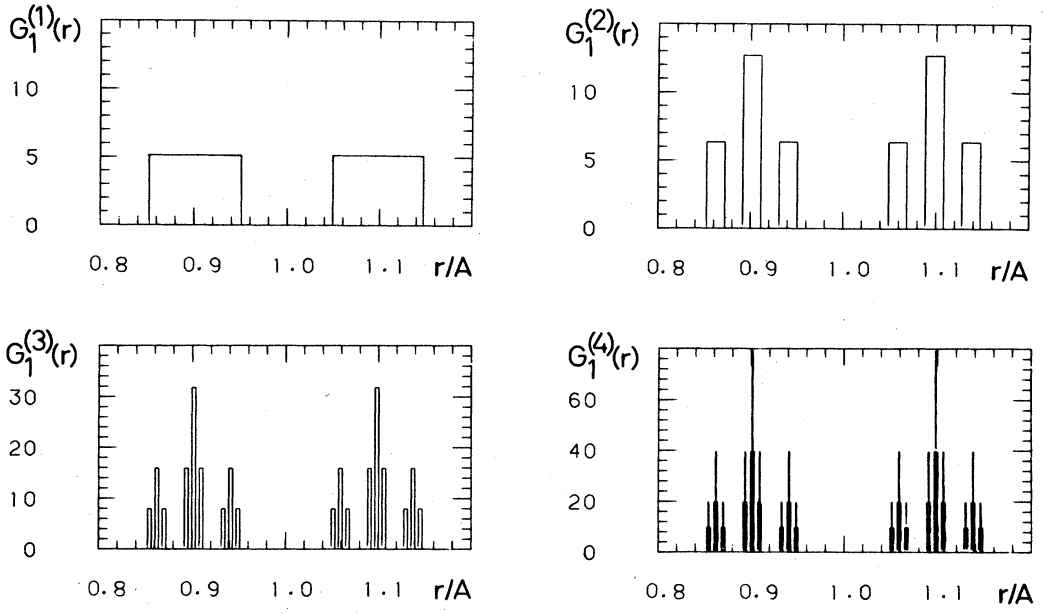

FIG. 4. Nearest-neighbor distribution function $G_1^{(\nu)}(r)$ for resolution $\nu=1,2,3,4$; $p=\frac{1}{2}$; and $\eta=0.2$.

and otherwise $G_1^{(\nu)}(r)=0$ and

$$\hat{\delta}_\nu=\frac{|\eta|^\nu}{1-|\eta|}\,, \tag{38c}$$

$\mu_0=\pm 1$, $\mu_i=0,\pm 1$ $(i\geq 1)$, and μ and μ' are the numbers of the $\mu_i (i\geq 1)$ which are zero and one, respectively. This result for $G_1^{(\nu)}(r)$ follows from (10a') taking into account that $\sigma_n=-1$ and 1 with probability $(1-p)$ and p, and $(\sigma_{n-i}+\sigma_{n+i})=-2$, 0, and $+2$ with probability $(1-p)^2$, $2p(1-p)$, and p^2, respectively. For $|\eta|<\frac{1}{3}$ all the intervals (38b) are disjoint.

$G_1^{(\nu)}$ is presented in Fig. 4 for $\nu=1,2,3,4$ and $p=\frac{1}{2}$ from which also the self-similarity becomes obvious. For an infinite resolution $G_1^{(\infty)}(r)=G_1(r)$ exists only in a distributive sense and consists of an infinite number of δ peaks with a Cantor set as support. For j small $G_j^{(\nu)}(r)$ is obtained in an analogous manner. However, for later purposes [calculation of $G(r)$ in the next section] we prefer another coarse graining than that of Fig. 4 where the resolution was related to η. Now we choose a resolution δ and denote by $G_j^{(\delta)}(r)$ the corresponding histogram of $G_j(r)$ with resolution δ (see Fig. 5 for $p=0.5$ and Fig. 6 for $p=0.3$ and two different δ). It is obvious that if δ is not correlated with η, the self-similarity does not manifest itself (compare Figs. 4 and 5 for $j=1$). Two properties follow from Figs. 5 and 6: (i) $p\neq\frac{1}{2}$ causes an asymmetry of $G_j^{(\delta)}(r)$ which is clear, and (ii) there is a qualitative difference between $G_j^{(\delta)}(r)$ for j even and j odd, that is, at $r=jA$ there is a peak or a gap for j even and j odd, respectively. This behavior is due to the special form of $V_1(x)$ consisting of *two* pieces of parabola which lead to two characteristic nearest-neighbor distances. We will come back to this point when we discuss the structure factor.

The asymptotic behavior of $G_j(r)$ for $j\to\infty$ can also be derived exactly. Using (10a') the jth-nearest-neighbor distance

$$D_j^n(\sigma)=\sum_{l=1}^{j} v_{n+l}(\sigma)$$

between atom n and atom $n+j$ can be rewritten as

$$D_j^n(\sigma)=jA+\frac{B}{2}\sum_{l=1}^{j}\sigma_{n+l}+R_j^n(\sigma)\,, \tag{39}$$

where

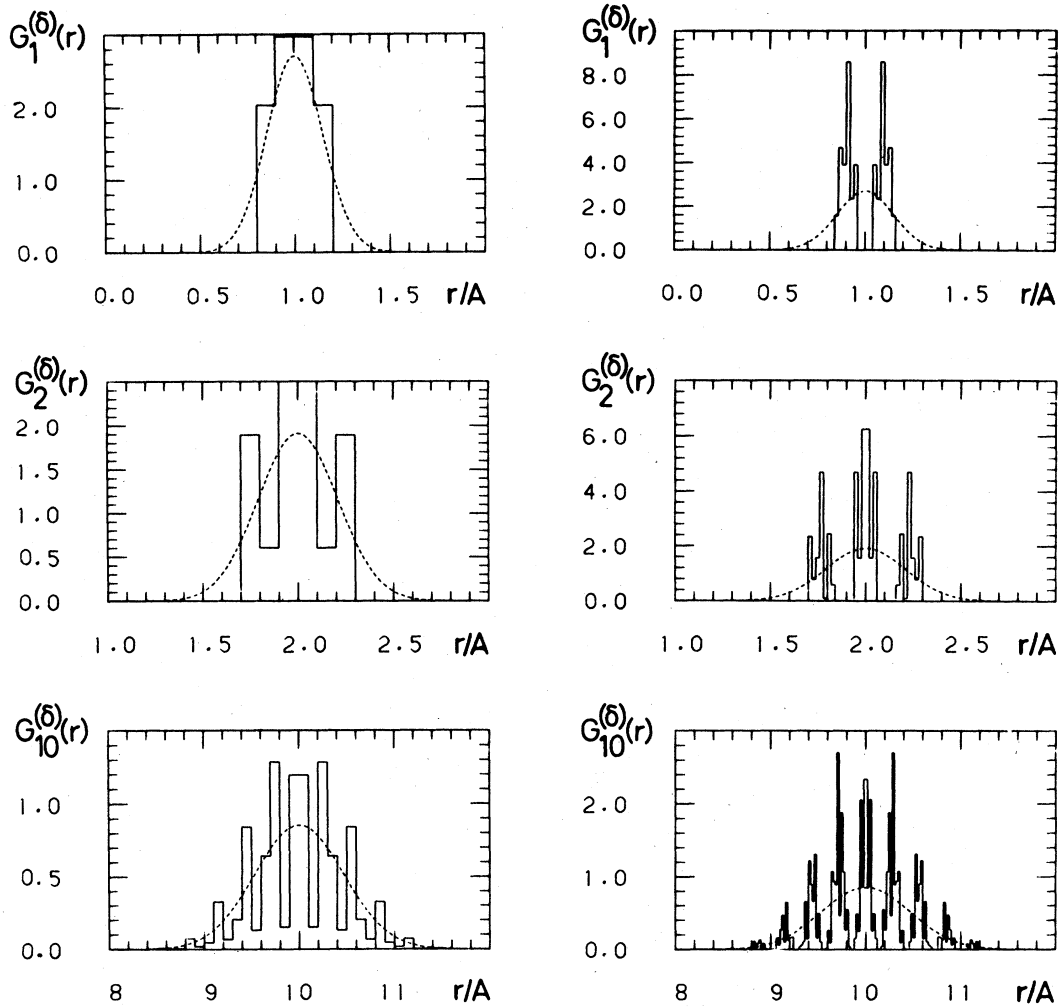

FIG. 5. Histogram $G_j^{(\delta)}(r)$ of the jth-nearest-neighbor-distribution function for $j=1$, 2, and 10, $\delta=0.1A$ (left column) and $\delta=0.02A$ (right column) and for $p=\frac{1}{2}$, $\eta=0.2$. The corresponding Gaussian distribution is represented by the dashed line.

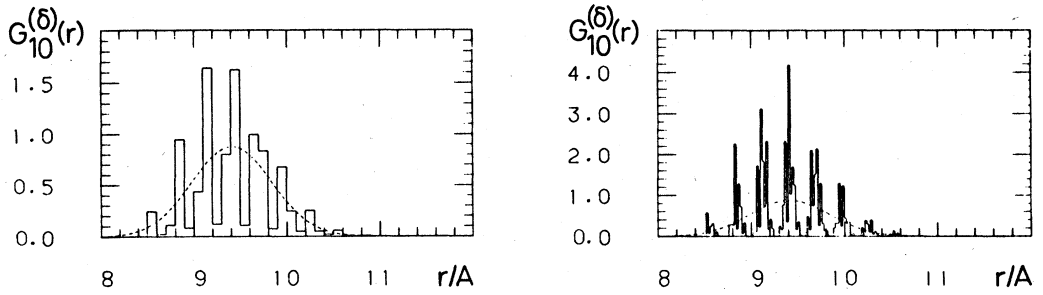

FIG. 6. Same as Fig. 5 but for $j=10$, $\delta=0.1A$ (left), and $\delta=0.02A$ (right) and for $p=0.3$, $\eta=0.2$.

$$\left|R_j^n(\sigma)\right|=\left|\frac{B}{2(1+\eta)}\sum_{i=1}^{\infty}\eta^i(\sigma_{n+i+j}-\sigma_{n+i}+\sigma_{n-i+1}-\sigma_{n-i+j+1})\right|\leq\frac{2B\,|\eta|}{(1+\eta)(1-|\eta|)} \tag{40}$$

is finite for all n, j, and σ, whereas $\sum_{l=1}^{j}\sigma_{n+l}$ takes values from $-j$ to $+j$. That $R_j^n(\sigma)$ is bounded will get crucial when we introduce a scaled variable which corresponds to $D_j^n(\sigma)/\sqrt{j}$, because then $R_j^n(\sigma)/\sqrt{j}$ vanishes asymptotically for $j\to\infty$. The p-normality of σ leads immediately to a binomial distribution for $\sum_{m=1}^{j}\sigma_{n+m}$, i.e.,

$$\lim_{N\to\infty}\left[\frac{1}{2N}\text{card}\left\{l\in\mathbb{Z}\mid -N\leq l<N \text{ and } \sum_{m=1}^{j}\sigma_{n+m+l}=2k-j\right\}\right]=p^k(1-p)^{j-k}\begin{bmatrix}j\\k\end{bmatrix} \tag{41}$$

(card is the cardinality of the set $\{\cdot\}$).

Using the fact that the rhs of (41) with an appropriate scaling converges to a Gaussian function, we get finally

$$\lim_{j\to\infty}\left[\frac{1}{A+(p-\frac{1}{2})B}\int_{r_1(j)}^{r_2(j)}dr\,G_j(r)\right]=\frac{1}{\sqrt{2\pi}}\int_{z_1}^{z_2}dz\,e^{-z^2/2}, \tag{42a}$$

where

$$r_i(j)=B\sqrt{p(1-p)j}\,z_i+j[A+(p-\tfrac{1}{2})B],\quad i=1,2\ . \tag{42b}$$

This equation states that the distribution function of the jth-nearest-neighbor distances scaled by $(B\sqrt{p(1-p)j}\,)^{-1}$ gets Gaussian as in I. However, there is a qualitative difference between the results for $G_j(r)$ in this paper, and those in I: In I also the unscaled functions $G_j(r)$ converged to a Gaussian distribution with a width $\sigma=(B/2)\sqrt{j}$, whereas here the G_j (which exist only in a distributive sense) and also the $G_j^{(\delta)}$ do not converge. In order to illustrate this we have also plotted in Figs. 5 and 6 the corresponding Gaussian function.

B. Pair distribution function

The pair distribution function for a one-dimensional configuration is given by

$$G(r)=\sum_{j=1}^{\infty}G_j(r)\ , \tag{43}$$

which exists only in a distributive sense because this is true for all $G_j(r)$. Therefore we consider again a coarse-grained function $G^{(\delta)}(r)$ which is presented in Fig. 7 for different δ. For high resolution more detailed structure appears due to the self-similarity of the G_j. For a fixed δ, the pair distribution function exhibits short-range order, i.e., there are more or less pronounced nearest-, next-nearest-, etc. neighbor peaks. At least for the lowest resolution, $G^{(\delta)}(r)$ (Fig. 7) seems to converge to unity from which one might conjecture that this property of the preceding model (I) may also hold for $G^{(\delta)}(r)$ of the present configurations. But this is not true in general. If B/A is rational, i.e.,

$$B/A=r/s\ , \tag{44}$$

r,s positive integers, all possible values of $D_j^n-R_j^n$ [see Eq. (41)] are contained in the set:

$$\{kA/2s\mid k\in\mathbb{Z}\}\ . \tag{45}$$

The possible values of R_j^n form a Cantor set which is bounded by (40) and which contains gaps of *finite* length. Therefore, there exist values R_1 and R_2 such that none of the intervals $[R_1+kA/2s,\ R_2+kA/2s]$, $k\in\mathbb{N}$ contains any possible particle distance. This disproves the convergence of $G^{(\delta)}(r)$ if the resolution is high enough. For B/A irrational we can prove

$$\lim_{r\to\infty}G^{(\delta)}(r)=1 \tag{46}$$

for all δ. This different behavior for rational and irrational values of B/A can be understood in the following way: according to (43) the set of all possible particle distances is the union of all possible jth-nearest-neighbor distances for $j=1,2,\ldots$, which are Cantor sets. The property of this superposition depends on B/A in a similar way as the distribution of the numbers $n\times B/A$ (mod 1), $n\in N$ in the unit intervals does. For B/A irrational this distribution is

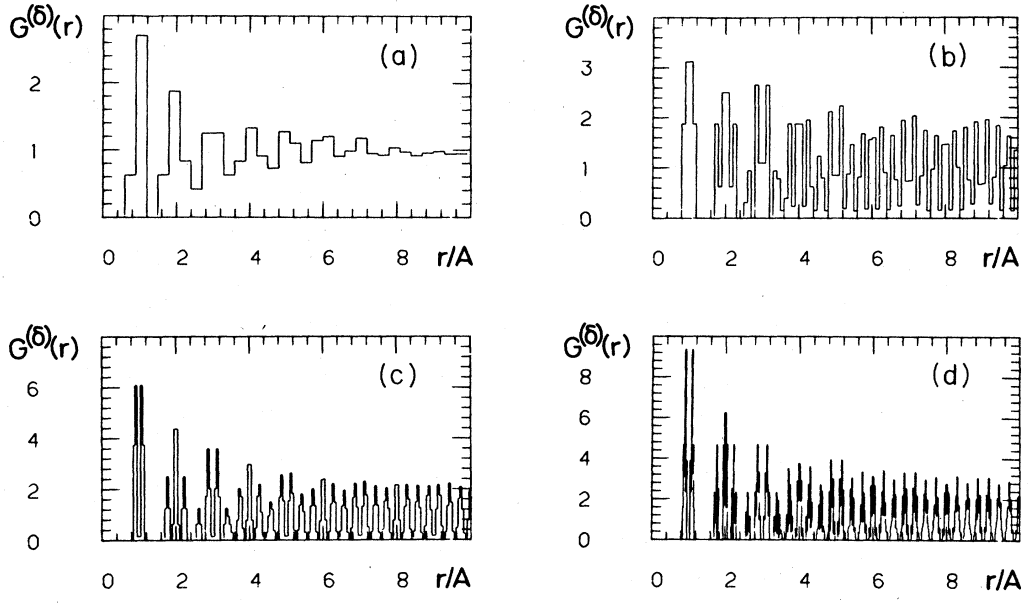

FIG. 7. Histogram $G^{(\delta)}(r)$ of the pair distribution function for (a) $\delta=0.3A$, (b) $0.1A$, (c) $0.05A$, and (d) $0.02A$; and for $p=\frac{1}{2}$, $\eta=0.2$.

uniform while it is discrete for B/A rational, i.e., there are gaps. It is just this discreteness which prevents the convergence of $G^{(\delta)}(r)$ for B/A a rational number. For B/A irrational where this does not occur we can prove Eq. (46) analogous to I.

C. Structure factor

The Fourier transform of $G^{(\delta)}(r)$ is just the coarse-grained structure factor or interference function $S^{(\delta)}(k)$ which is shown in Fig. 8 for $G^{(\delta)}(r)$ given in Fig. 7(c). There is a peculiarity not observed in experimental results for three-dimensional disordered solids: Besides the normal peaks at $k_n=n\times 2\pi/[A+(p-\frac{1}{2})B]$ there exist also peaks at $k_n'=(n-\frac{1}{2})\times 2\pi/[A+(p-\frac{1}{2})B]$ and at $k_n''=(n/2)\times 2\pi/A$ for $n\geq 1$. The peaks at k_7'' and at k_{14}'' can easily be identified in Fig. 7.

These additional peaks point out the existence of at least two more characteristic lengths which originate from the fact that $G^{(\delta)}(r)$ differs for j even and j odd as already discussed.

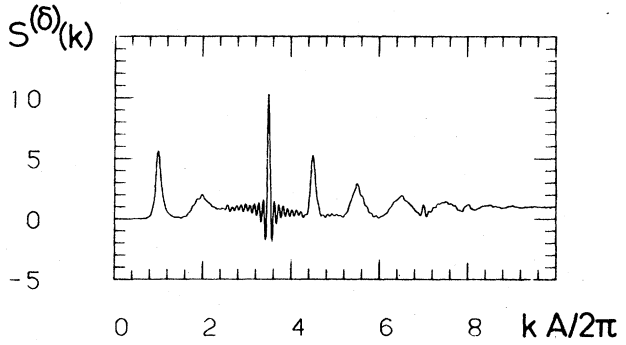

FIG. 8. Interference function $S^{(\delta)}(k)$ for the pair distribution function of Fig. 7(c).

V. TWO-LEVEL SYSTEMS AND SPECIFIC HEAT

Now we show that for each chaotic configuration $\{v_n(\sigma)\}$ with energy $E(\sigma)$ there exist a set of other chaotic configurations $\{v_n(\sigma')\}$ with energy $E(\sigma')$ where each σ' differs from σ only locally. $\{v_n(\sigma')\}$ is connected to $\{v_n(\sigma)\}$ over a potential barrier $V(\sigma,\sigma')$. The transition $\sigma\rightarrow\sigma'$ represents the excitation of a two-level system with classical excitation energy (also called asymmetry):

$$\Delta(\sigma,\sigma')=E(\sigma)-E(\sigma')\ , \tag{47}$$

which may be positive or negative on account of the metastability of the configuration $\{v_n(\sigma)\}$. In the following we always assume σ to be p-normal. (We have slightly changed the notation with respect to II, thus adopting the usual one, e.g., Ref. 11).

A. Two-level systems

Because the two-level systems are expected to be localized one must have

$$\sum_n(\sigma_n-\sigma_n')=0\ . \tag{48}$$

Using (48) we get from (10a') that

$$\sum_n[v_n(\sigma)-v_n(\sigma')]=0\ , \tag{49}$$

i.e., the length of the chain remains unchanged during a transition $\sigma\rightarrow\sigma'$. The simplest transition for which (48)

holds is the following: Let $i-1$ and i be such bonds for which $\sigma_{i-1}=-\sigma_i$. Then we choose $\sigma'_{i-1}=\sigma_i$, $\sigma'_i=\sigma_{i-1}$ and $\sigma'_n=\sigma_n$ for all $n\neq i-1,i$. The new metastable chaotic configuration $\{v_n(\sigma')\}$ is obtained from $\{v_n(\sigma)\}$ just by moving the ith particle over a potential barrier with all the other particles fixed and then relaxing the chain. Although σ and σ' differ only for two bonds, the nearest-neighbor distances $v_n(\sigma)$ and $v_n(\sigma')$ of course differ for all n but converge to each other for $n\to\pm\infty$ (see Fig. 9). From (10a') we get

$$v_n(\sigma)-v_n(\sigma')=\sigma_i 2B(1-\eta)\begin{cases}-\eta^{i-1-n}, & n\leq i-1\\ \eta^{n-i}, & n\geq i\end{cases} \tag{50}$$

which shows that $|v_n(\sigma)-v_n(\sigma')|$ decreases exponentially with the "distance" $|i-n|$ and that it is not only one atom which changes its position but a group of atoms, the number of which is determined by $|\eta|$. The energy $\Delta_i(\sigma)$ of these two-level systems which we characterize symbolically by

$$(1,-1)\leftrightarrow(-1,1) \tag{51}$$

follows straightforward from (24) and (47):

$$\Delta_i(\sigma)=\sigma_i 4J_0(1-\eta)\sum_{n=1}^{\infty}\eta^n(\sigma_{i+n}-\sigma_{i-1-n})\ . \tag{52}$$

For more complicated transitions, e.g.,

$$(1,-1,1,-1)\leftrightarrow(-1,1,-1,1)\ , \tag{53}$$

the energy of the corresponding two-level systems can also be calculated exactly, but now more particles have to move. This means that the effective mass of the tunneling group of atoms is increased, which implies rather long relaxation times. Therefore their contribution to the low-temperature specific heat can be neglected on a time scale much smaller than the corresponding relaxation time. In any case the discussion shows that there exists a *hierarchy* of two-level systems classified by the number of particles which are moved.

If we consider a transition for which (48) is not true, e.g., $\sigma_i=1(-1)$, $\sigma'_i=-\sigma_i$, and $\sigma'_n=\sigma_n$ for all $n\neq i$ it is no longer possible to choose, e.g., $u_0(\sigma')$ such that asymptotically for $n\to\pm\infty$ the particle positions $u(\sigma')$ and $u_n(\sigma)$ converge to each other. Therefore this type of transition is a *nonlocalized* excitation.

The Δ_i [Eq. (52)] form a spectrum which is a Cantor set symmetric to zero. This we will see when discussing the density of states.

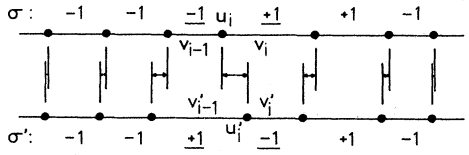

FIG. 9. Comparison of two configurations $\{v_n(\sigma)\}$ and $\{v'_n=v_n(\sigma')\}$ for $\sigma_{i-1}=\sigma'_i=-\sigma_i=-\sigma'_{i-1}$ and $\sigma_n=\sigma'_n$, $n\neq i-1,i$. The vertical bars illustrate the difference between the particle positions of both configurations.

B. Potential barriers

In order to calculate the potential barriers $V(\sigma,\sigma')$ separating the configurations $\{v_n(\sigma)\}$ and $\{v_n(\sigma')\}$ we add external forces which change $\{v_n(\sigma)\}$ continuously into $\{v_n(\sigma')\}$. The potential barrier is then obtained from the work done by the external forces. Considering only two-level systems of type (51), we add to Eq. (1):

$$-F(u_i-u_{i-1})-F'(u_{i+1}-u_i) \tag{54}$$

and determine the equilibrium configurations for fixed F and F'. These are solutions of

$$\frac{\partial V}{\partial u_n}=-F\delta_{i-1,n}+(F-F')\delta_{i,n}+F'\delta_{i+1,n}\ . \tag{55}$$

Using (3) and (55) we get for the function I [Eq. (4)], which is no longer an invariant because the symmetry (2b) is broken:

$$\begin{aligned}&I(v_{i-2},v_{i-1},v_i)=F\ ,\\ &I(v_{i-1},v_i,v_{i+1})=F'\ ,\\ &I(v_{n-1},v_n,v_{n+1})=0\ \text{ for } n\neq i-1,i\ ,\end{aligned} \tag{56}$$

which yield the modified difference equation:

$$2\gamma v_n+v_{n-1}+v_{n+1}=\phi(v_n)+F\delta_{i-1,n}+F'\delta_{i,n}\ . \tag{57}$$

This equation can easily be solved if

$$\sigma_n(F,F',\sigma)\equiv\mathrm{sgn}[v_n(F,F',\sigma)-c]=\sigma_n \tag{58}$$

for all n, i.e., the quenched-bond disorder remains unchanged under the action of the external forces which can only be true if F and F' are small enough. Substituting the ansatz,

$$v_n(F,F',\sigma)=v_n(\sigma)+w_n(F,F')\ , \tag{59}$$

into (57), we get a *linear* but inhomogeneous difference equation for w_n [if we assume (58)]:

$$2\gamma w_n+w_{n+1}+w_{n-1}=F\delta_{i-1,n}+F'\delta_{i,n}\ , \tag{60}$$

with the solution:

$$w_n(F,F')=\begin{cases}w_0(F,F')\eta^{i-1-n}, & n\leq i-1\\ w_0'(F,F')\eta^{n-i}, & n\geq i\end{cases} \tag{61a}$$

where the variations w_0 and w_0' of the nearest-neighbor distances v_{i-1} and v_i, respectively, are given by

$$\begin{aligned}&w_0(F,F')=\frac{1}{C_1}\frac{1+\eta}{1-\eta}(F+\eta F')\ ,\\ &w_0'(F,F')=w_0(F',F)\ .\end{aligned} \tag{61b}$$

One can show[27] that there exists a range for (a_1,a_2,c,b) such that (58) is satisfied for all n if $|\eta|<\frac{1}{3}$ and if $\sigma_n(F,F',\sigma)=\sigma_n$ for $n=i-1,i$, where the latter condition restricts F and F' such that

$$\begin{aligned}&0\leq|w_0(F,F')|<|\delta_{i-1}|\ ,\\ &0\leq|w_0'(F,F')|<|\delta_i|\end{aligned} \tag{62a}$$

with

$$\delta_n = v_n(\sigma) - c \ . \tag{62b}$$

Now we can calculate the barrier heights $b_i(\sigma)$ with respect to the energy level $E(\sigma)$:

$$b_i(\sigma) = \int_{(0,0)}^{(\delta_{i-1},\delta_i)} [dw_0 F(w_0,w_0') + dw_0' F'(w_0,w_0')] \ , \tag{63}$$

where the line integral is path independent. Substituting $F(w_0,w_0')$ and $F'(w_0,w_0')$, which follow from (61b), into (63), we get finally

$$b_i(\sigma) = \frac{C_1}{2}(1+\eta)^{-2}([v_{i-1}(\sigma)-c]^2 - 2\eta[v_{i-1}(\sigma)-c][v_i(\sigma)-c] + [v_i(\sigma)-c]^2) \ . \tag{64}$$

The barrier $b_i'(\sigma)$ with respect to $E(\sigma')$ follows similarly and is related to $b_i(\sigma)$ by

$$b_i'(\sigma) = b_i(\sigma) - \Delta_i(\sigma) = b_i(\sigma') \ . \tag{65}$$

Thus the potential barriers V_i (defined as usual, e.g., Ref. 11) are

$$V_i(\sigma) = [b_i(\sigma) + b_i'(\sigma)]/2 = b_i(\sigma) - \Delta_i(\sigma)/2 \ . \tag{66}$$

A straightforward but laborious estimation[27] leads to the following upper and lower bounds for $V_i(\sigma)$ for *all* $|\eta| < \frac{1}{3}$, *all* σ and *all* i:

$$V_{\min}(\eta) < V_i(\sigma) < V_{\max}(\eta) \tag{67a}$$

with

$$V_{\min}(\eta) \geq \tfrac{2}{3} C_1 a_-^{\,2}, \quad V_{\max} \leq \tfrac{7}{3} C_1 a_-^{\,2} \ . \tag{67b}$$

For $|\eta| \ll 1$ this estimation is, however, rough: For $|\eta| \ll 1$ it follows from (37) that the nearest-neighbor distances $v_{i-1}(\sigma)$ and $v_i(\sigma)$ deviate little from $A \mp B/2$ and $A \pm B/2$ where the upper and lower sign holds for $\sigma_i = 1$ and $\sigma_i = -1$, respectively, and therefore $b_i(\sigma)/C_1$ [Eq. (64)] cannot fluctuate much, and in particular one has

$$\lim_{\eta \to 0} V_{\max}(\eta)/V_{\min}(\eta) = 1 \ . \tag{68}$$

The bounds in (67) can be improved if one treats $\eta > 0$ and $\eta < 0$ separately. We have found that $V_{\max}(\eta)/V_{\min}(\eta) \leq \frac{7}{4}$ and ≤ 3 for $\eta > 0$ and $\eta < 0$, respectively. In any case the highest and lowest potential barrier are of the same order.

Finally we note that the barriers b_i or V_i are not distributed continuously, but form a Cantor set as the v_i do.

C. Correlations between the asymmetries Δ_i and the potential barriers V_i

The role of the correlations between the classical energies Δ_i (asymmetry) and the potential barriers V_i have been discussed by Phillips.[6] For our model the potential barriers for those two-level systems with energy smaller than 10^{-4} eV (later we consider only those for the specific heat below 1 K) are weakly correlated with Δ_i, and the correlations even go to zero for such asymmetries Δ_i which get arbitrarily small. This can be seen as follows: From (52) it is obvious that for such i with $\Delta_i(\sigma) < C_1 a_-^{\,2} \eta^\nu$ one must have

$$\sigma_{i+n} = \sigma_{i-1-n} \quad \text{for } 1 \leq n < \nu \ . \tag{69}$$

Using (69) and $\sigma_{i-1} = -\sigma_i$ (which characterizes the two-level systems we are discussing) we get from (10a'):

$$v_{i-1}(\sigma) = A + \frac{B}{2}\frac{1-\eta}{1+\eta}\left[-(1-\eta)\sigma_i + (1+\eta)\sum_{n=1}^{\nu-1}\eta^n\sigma_{i+n} + O(\eta^\nu)\right], \tag{70}$$

$$v_i(\sigma) = A + \frac{B}{2}\frac{1-\eta}{1+\eta}\left[(1-\eta)\sigma_i + (1+\eta)\sum_{n=1}^{\nu-1}\eta^n\sigma_{i+n} + O(\eta^\nu)\right] .$$

Thus, the distribution of $[v_{i-1}(\sigma)-c]$ and $[v_i(\sigma)-c]$ and therefore also the distribution of the barriers $b_i(\sigma)$ [Eq. (64)] and V_i, respectively, is mainly determined by all possible subsequences $\{\sigma_i, \sigma_{i+1}, \ldots, \sigma_{i+\nu-1}\}$, whereas the asymmetries $\Delta_i(\sigma)$ below $C_1 a_-^{\,2}\eta^\nu$ do *not* depend on these subsequences. The remainder of the sequence σ, i.e., σ_{i-1-n} and σ_{i+n} for $n \geq \nu$ which determine the asymmetries and their distribution below $C_1 a_-^{\,2}\eta^\nu$ uniquely, influence the barrier heights only on an energy scale of order $C_1 a_-^{\,2}\eta^\nu$, as follows from (64) and (70). Therefore, assuming that the barriers are of order 10^{-1} eV with variations restricted roughly by (67), the asymmetries which are smaller than $C_1 a_-^{\,2}\eta^\nu = 10^{-4}$ eV influence the barriers only on a scale of 10^{-4} eV which can be neglected with respect to the scale of 10^{-1} eV.

D. Quantum corrections

Because we will discuss the behavior of the specific heat below 1 K we have to estimate the quantum corrections. The corrected energies of the two-level systems are given by[5,6]

$$\Delta_i^{qm}(\sigma) = \{(\Delta_i(\sigma) + \tfrac{1}{2}[\hbar\omega_0(\sigma) - \hbar\omega_0(\sigma')])^2 + \Delta_{0,i}^2\}^{1/2} \ , \tag{71a}$$

where $\frac{1}{2}\hbar\omega_0(\sigma)$ is the zero-point energy of an equilibrium configuration characterized by σ, and σ' follows from σ just by interchanging σ_{i-1} and $\sigma_i = -\sigma_{i-1}$ (see above). As we have seen in Sec. III, the phonon frequencies $\omega(q)$ and therefore $\hbar\omega_0$ given by

$$\hbar\omega_0 = \frac{1}{2\pi}\int_0^{2\pi} dq\, \hbar\omega(q) \tag{71b}$$

do not depend on σ. Thus the term $\frac{1}{2}[\hbar\omega_0(\sigma) - \hbar\omega_0(\sigma')]^2$

in (71a) just vanishes. $\Delta_{0,i}$ is the overlap between the wave functions in both local energy minima and is approximately given by

$$\Delta_{0,i} \approx \hbar\omega_0 \exp(-\lambda_i) , \quad \lambda_i \approx \tfrac{1}{2}(2MV_i)^{1/2} l/\hbar , \tag{71c}$$

where l is a typical tunneling distance and M the total mass of the tunneling unit which may consist of more than one atom. The zero-point energy does not depend sensitively on η and is well approximated by[27]

$$\tfrac{1}{2}\hbar\omega_0 \approx \tfrac{1}{2}\hbar(C_1/m)^{1/2} . \tag{72}$$

In the following we estimate $\Delta_{0,i}$ and the rate Γ_i of the transitions (51) which is roughly of the form:

$$\Gamma_i \approx \Gamma_0 \exp(-2\lambda_i) , \tag{73a}$$

where

$$\Gamma_0 \approx \omega_0 . \tag{73b}$$

For this estimation we assume

$$V_{\max} \approx 10^{-1} \text{ eV} , \quad l = a_- \approx 1 \text{ Å} , \quad m = M \approx 16 \text{ u (oxygen atom)} . \tag{74}$$

If we use the rhs of (67) for $V_{\max}$ we get $C_1 \approx 650$ g sec^{-2}, which leads to a zero-point energy:

$$\tfrac{1}{2}\hbar\omega_0 \approx 1.5 \times 10^{-3} \text{ eV} . \tag{75}$$

The maximum value for $\Delta_{0,\max}$ follows from (71c) for $\lambda_i = \lambda_{\min}$. Using for $V_{\min} \approx \frac{1}{3} V_{\max}$ we get $\lambda_{\min} \approx 8.5$ which leads to

$$\Delta_{0,\max} \approx 5 \times 10^{-7} \text{ eV} , \tag{76}$$

which can be neglected for those asymmetries Δ_i in the range 10^{-5} eV and larger. Because

$$\lambda_{\max} = (V_{\max}/V_{\min})^{1/2} \lambda_{\min} \approx 14.5$$

we find that

$$\Gamma_{\min} \approx 1 \text{ sec}^{-1} . \tag{77}$$

These estimations demonstrate that, e.g., for the set of data given by (74) the resonant tunneling can be neglected on a scale of 10^{-5} eV and larger, i.e., in this regime the asymmetries Δ_i are the approximate two-level energies.

E. Density of states $n(\epsilon)$ and specific heat

We approximate $n(\epsilon)$ by the distribution function of the asymmetries Δ_i which is justified for $\epsilon > \approx 10^{-5}$ eV as we have seen before. Then $n(\epsilon)$ can be obtained quite similarly from Δ_i [Eq. (52)] as $G_1(r)$ [see Eq. (38)] followed from the v_i's [Eq. (10a')]. Thus for an energy resolution of order $\epsilon_0 \eta^\nu$ [$\epsilon_0 = 8 \mid J_0 \eta \mid (1-\eta)$] we find for the νth order density of states $n_\nu(\epsilon)$:

$$n_\nu(\epsilon) = n_0 \begin{cases} [p(1-p)]^{\nu-\mu}[p^2+(1-p)^2]^\mu \mid \eta \mid^{-\nu}, & \text{for } \epsilon \in I_{\mu_1,\mu_2,\ldots,\mu_\nu} \\ 0 & \text{otherwise} , \end{cases} \tag{78a}$$

where

$$I_{\mu_1 \cdots \mu_\nu} = \left[\epsilon_0 \left[\sum_{i=1}^{\nu} \mid \eta \mid^{i-1} \mu_i - \delta_\nu \right] , \epsilon_0 \left[\sum_{i=1}^{\nu} \mid \eta \mid^{i-1} \mu_i + \delta_\nu \right] \right] , \quad \mu_i = 0, \pm 1$$

$$\delta_\nu = \mid \eta \mid^\nu / (1 - \mid \eta \mid) , \quad n_0 = (1 - \mid \eta \mid) p(1-p) \epsilon_0^{-1} , \tag{78b}$$

and μ is the number of μ_i's which are zero. Here we have taken into account that for N particles there are $2p(1-p) \times N$ two-level systems (if σ is p-normal). For $p = \frac{1}{2}$, Eqs. (78) reduce to the result in II. $n_\nu(\epsilon)$ is shown in Fig. 10 for $p = \frac{1}{3}$. From (78) we find the scaling property:

$$n_{\nu+1}(\mid \eta \mid \epsilon) = [p^2+(1-p)^2] \mid \eta \mid^{-1} n_\nu(\epsilon) , \tag{79}$$

for $\mid \epsilon \mid \leq \epsilon_0 (1 - \mid \eta \mid)^{-1}$ and $\nu \geq 1$. This and also the Cantor set structure ($\nu \to \infty$) of the two-level energies become obvious from Fig. 10. It is quite remarkable that we obtain a Cantor spectrum with self-similarity for the two-level systems of a *disordered* configuration. That such a Cantor spectrum can be obtained for the vibrational modes of a *fractal*[25] was recently demonstrated by Alexander and Orbach[29] and Rammal,[30] but there the self-similarity is already included in the atomic arrangement. For the fractal dimension[25] $\hat{d}$ of our Cantor spectrum we get:

$$\hat{d} = \ln(1/3)/\ln \mid \eta \mid , \tag{80}$$

which is smaller or equal to 1 for $\mid \eta \mid \leq \frac{1}{3}$. The spectral dimension $\tilde{d}$ introduced by Rammal and Toulouse[31] is defined by

$$n(\epsilon) \sim \epsilon^{\tilde{d}-1}, \quad \epsilon \to 0 , \tag{81}$$

and can be obtained from (79) (for $\nu \to \infty$) which yields

$$\tilde{d} = \ln[p^2+(1-p)^2]/\ln \mid \eta \mid = \hat{d} \ln[p^2+(1-p)^2]/\ln(\tfrac{1}{3}) . \tag{82}$$

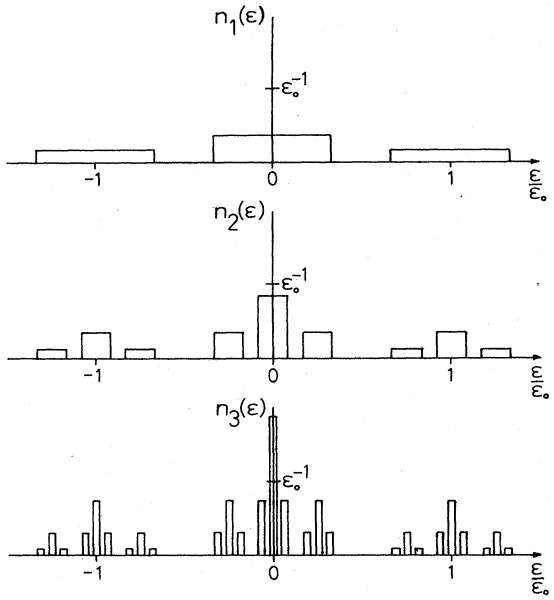

FIG. 10. Density of states $n_\nu(\epsilon)$ for $\nu=1$, 2, and 3 and $p=\frac{1}{3}$, $|\eta|=\frac{1}{4}$.

If we use the power-law behavior (81) for the density of states we obtain for the specific heat $c(T)$:

$$c(T)\sim T^{\tilde{d}}\,, \tag{83}$$

which holds, however, only for temperatures of the order 10^{-5} eV or larger because only then the distribution of the Δ_i's approximates well the density of states. For these considerations we have assumed (i) that all two-level systems contribute to the specific heat, which is only true if the time scale of the specific-heat measurement is much larger than $\Gamma_{\min}^{-1}=1$ sec [Eq. (77)], and (ii) that the correlations between the two-level systems and the barriers can be neglected which is true for energies smaller than $\approx 10^{-4}$ eV which correspond to 1 K. Therefore in a range between 0.1 and 1 K the specific heat of the two-level systems (phonons excluded) should be given by (83) with a fractional exponent $\tilde{d}<0.63$ if the time scale of the measurement is much larger than 1 sec. $\tilde{d}$ depends only on the type of quenched bond disorder characterized by p and on the ratio of the elastic constants C_1/C_2.

VI. GENERALIZATION OF THE MODEL

We have already discussed (in Sec. III F) a possible generalization of the model (1) with interaction potential V_1 and V_2 given by Eqs. (6). We have found that the results obtained with (6) change smoothly if we add further anharmonic interaction to V_1. In particular we could also smoothen the cusp in V_1 because for $|\eta|<\frac{1}{3}$ [and (a_1,a_2,c,b) in a suitable range] all the nearest-neighbor distances of the equilibrium configurations (10a') avoid the neighborhood of c (the location of the cusp). This neighborhood increases with decreasing $|\eta|$. Then (10a') still represents metastable equilibrium configurations, but there may exist additional ones. Further generalizations would be the use of anharmonic next-nearest-neighbor interactions or that of harmonic third-, etc. neighbor potentials. These types of generalization we have not discussed yet. We mention here a different kind of generalization: The potential energy (1) is *not* of the form of a sum of pair potentials, and the interaction between two particles i and j in the chain depends on the number of particles situated between u_i and u_j, which constitutes a many-body interaction. We have found, however, a pair potential $V_p(|u_i-u_j|)$ for which the stationary configurations (10a') remain metastable equilibrium configurations. V_p can be derived as follows: Let $\underline{v}$ and $\overline{v}$ denote the minimum and maximum nearest-neighbor distance, respectively, following from (10a'). Then, if the first-, second-, and third-nearest-neighbor distances do *not* overlap, which holds if

$$\overline{v}<2\underline{v}\,, \tag{84a}$$

$$2\overline{v}<3\underline{v} \tag{84b}$$

[(84b) implies (84a)], both potentials V_1 and V_2 can be joined to a pair potential:

$$V_p(x)=\begin{cases} V_1(x)+k_1, & x\in[\underline{v},\overline{v}]\,, \\ V_2(x)+k_2, & x\in[2\underline{v},2\overline{v}]\,, \\ 0, & x\in[3\underline{v},\infty]\,, \end{cases} \tag{85}$$

with arbitrary constants k_i. Within the intervals $(0,\underline{v})$, $(\overline{v},2\underline{v})$, and $(2\overline{v},3\underline{v})$, we can choose V_p, arbitrarily. That one can easily find parameters a_1, a_2, c, b, and η for which (84) is fulfilled is demonstrated by Fig. 11, which shows a pair potential being in good qualitative agreement with pair potentials obtained from scattering data of liquids by, e.g., see Schommers.[32] If we would still smoothen the cusp at c (which we are allowed to do for $|\eta|<\frac{1}{3}$) our pair potential would just exhibit the shoulder of the potential given in Ref. 32. That $V_p(x)$ vanishes for $x>3\underline{v}$ may not be serious, for instance, an exponen-

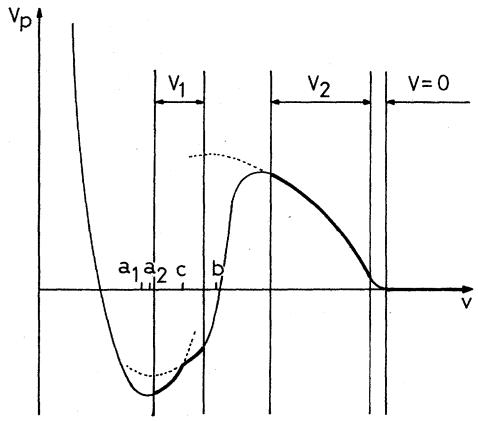

FIG. 11. Pair potential $V_p(v)$. V_1 and V_2 denote the part of the nearest- and next-nearest-neighbor potential.

tially decaying tail for $x > 3\underline{v}$ may not influence our results much.

In any case for a certain class of *pair potentials,* Eq. (85), we have proved the existence of chaotic, metastable equilibrium configurations at $T=0$ K with properties described in the preceding sections.

VII. DISCUSSION

Although the one-dimensional model we have studied in this paper is *translationally invariant* it has an infinite number of *chaotic* and *metastable* equilibrium configurations. This demonstrates that competing and anharmonic interactions, which induce frustration effects, may lead to glasslike locally stable configurations ($T=0$ K) classified by sequences $\{\sigma_n\}$ (p-normal) which characterize the type of quenched bond disorder. The fact that the equilibrium configurations are uniquely determined by $\{\sigma_n\}$ is related to the embedding of the Bernoulli shift into a map, the orbits of which correspond to the equilibrium configurations of the chain. This situation is independent on the different shapes of V_1 (see Fig. 1) and does not change under small perturbations like further anharmonicities of V_1. We have further demonstrated the existence of pair potentials for which our chaotic configurations remain metastable equilibrium configurations.

The pair distribution function $G(r)$ for these chaotic particle arrangements shows roughly a glasslike behavior, i.e., more or less pronounced nearest-, next-nearest-, etc., neighbor peaks and the absence of long-range order, but each of these peaks itself can be resolved into finer peaks, which is related to the bizarre and noncontinuous distribution of the nearest-neighbor distances. This is not observed in experiments, for which there may be several reasons: (i) for finite temperatures the bizarre structure of $G(r)$ will be smeared out; (ii) usually the radial distribution function (averaged over the angles) is obtained, and this only in an indirect way from the interference function which can be measured only with a certain accuracy; and (iii) we cannot exclude the possibility that this behavior is specific to one dimension. The extra peaks appearing in the interference function $S(k)$ originate from the existence of two typical nearest-neighbor distances (classified by $v_n > c$ and $v_n < c$) in our model. These peaks should be observable for a chain with two species of different equilibrium length.

Our model also allows a microscopic justification of the tunneling- or two-level systems. They are localized and involve a finite number of particles which tunnel through a potential barrier. These barriers and the energies of the simplest (where the smallest number of particles are involved) two-level systems which themselves are part of a hierarchy of two-level systems, we have calculated exactly. The corresponding density of states is *not* constant, as assumed in previous models, and it exhibits a scaling property as a result of the Cantor spectrum formed by the two-level systems which leads to a power-law behavior $c(T) \sim T^{\tilde{d}}$ for the specific heat (only two-level systems) between 0.1 and 1 K for measurements with time scale larger than 1 sec.

The fractional exponent $\tilde{d}$ is nonuniversal and depends only on $|\eta|$ related to C_1/C_2, the ratio of the elastic constants of the nearest- and next-nearest-neighbor interactions, and also on p which characterizes the type of quenched bond disorder. $\tilde{d}$ tends to zero for either $p \to 0$ or $p \to 1$ which corresponds to a situation where one of the two typical bond lengths is dilute and which is therefore comparable to the system studied by Geszti.[14] This behavior implies that $\tilde{d}$ *decreases* under annealing for the case where the ground state of the chain corresponds to $p=0$ or $p=1$ and $\tilde{d}$ *increases* for a glasslike configuration with $p \neq \frac{1}{2}$ if the ground state is of period two. For our model $0 < \tilde{d} < \ln 2/\ln 3 \cong 0.63$. Such exponents smaller than one are observed (see, e.g., Ref. 8) for three-dimensional solids. Because, however, the two-level systems are localized excitations, their density of states and therefore $\tilde{d}$ possibly does not depend sensitively on the Euclidean dimension. Specific heat and thermal conductivity measurements on β aluminia (a quasi-two-dimensional system) by Anthony and Anderson[33] lead to similar exponents (< 1 K) as for three-dimensional amorphous solids which support the conjecture. Therefore one may find similar results for two- and three-dimensional models.

But, on the other hand, there exist layered compounds or quasi-one-dimensional systems to which our model may apply. For instance, the polymer chains investigated in Ref. 18 which expand inhomogeneously under a tension such that the chain consists of two types of elements of different lengths might be modeled by the double-well-like potential V_1 of Fig. 1.

In conclusion we can say that the one-dimensional chaotic configurations we have investigated show, besides typical glasslike properties, some peculiarities which may or may not be specific to one dimension.

ACKNOWLEDGMENTS

We are grateful to Professor H. Thomas for many valuable comments concerning the presentation of this paper. This work was supported in part by the Swiss National Science Foundation.

[1]J. A. Barker, M. R. Hoare, and J. L. Finney, Nature (London) **257**, 120 (1975).

[2]P. Steinhardt, R. Alben, and D. Weaire, J. Noncryst. Solids **15**, 199 (1974).

[3]See, e.g., *Proceedings of the International Conference on "Order in Chaos,"* edited by D. Campbell and H. Rose [Physica D, **7** (1983)].

[4]R. C. Zeller and R. O. Pohl, Phys. Rev. B **4**, 2029 (1971).

[5]P. W. Anderson, B. I. Halperin, and C. M. Varma, Philos. Mag. **25**, 1 (1972).

[6]W. A. Phillips, J. Low Temp. Phys. **7**, 351 (1972).

[7]J. C. Lasjaunias, A. Ravex, M. Vandorpe, and S. Hunklinger,

Solid State Commun. **17**, 1045 (1975).
[8]J. C. Lasjaunias and A. Ravex, J. Phys. F **13**, L101 (1983).
[9]A. Ravex, J. C. Lasjaunias, and O. Béthoux, Physica **107B**, 397 (1981).
[10]M. Meissner and K. Spitzmann, Phys. Rev. Lett. **46**, 265 (1981).
[11]*Amorphous Solids: Low Temperature Properties,* edited by W. A. Phillips (Springer, Berlin, 1981).
[12]L. W. Molenkamp and D. A. Wiersma, J. Chem. Phys. (to be published).
[13]L. Pietronero and S. Strässler, Phys. Rev. Lett. **42**, 188 (1979).
[14]T. Geszti, Phys. Rev. B **30**, 1811 (1984).
[15]N. Rivier and D. M. Duffy, J. Phys. (Paris) **43**, 293 (1982).
[16]P. Reichert and R. Schilling, Phys. Rev. B **30**, 917 (1984); J. Math. Phys. **26**, 1165 (1985).
[17]R. Schilling, Phys. Rev. Lett. **53**, 2258 (1984).
[18]R. Bonart, Prog. Colloid Polym. Sci. **58**, 36 (1975).
[19]See, e.g., *Topological Disorder in Condensed Matter,* edited by F. Yonezawa and T. Ninomiya (Springer, Berlin, 1983).
[20]T. Janssen and J. A. Tjon, J. Phys. A **16**, 673 (1983).
[21]J. Villain and M. B. Gordon, J. Phys. C **13**, 3117 (1980).
[22]F. Axel and S. Aubry, J. Phys. C **14**, 5433 (1981).
[23]V. I. Arnold and A. Avez, *Ergodic Problems in Classical Mechanics* (Benjamin, New York, 1968).
[24]S. Smale, Bull. Am. Math. Soc. **73**, 747 (1967).
[25]B. B. Mandelbrot, *The Fractal Geometry of Nature* (Freeman, San Francisco, 1982).
[26]S. Aubry, in *Physics of Defects,* edited by R. Balian, M. Kléman, and J.-P. Poirier (North-Holland, Amsterdam, 1981).
[27]P. Reichert, Ph.D. dissertation (University of Basel, 1985).
[28]I. Niven, *Irrational Numbers, The Carus Mathematical Monograph 11* (Wiley, New York, 1956).
[29]S. Alexander and R. Orbach, J. Phys. (Paris) Lett. **43**, L625 (1982).
[30]R. Rammal, J. Phys. (Paris) **45**, 191 (1984).
[31]R. Rammal and G. Toulouse, J. Phys. (Paris) Lett. **44**, L13 (1983).
[32]W. Schommers, J. Noncryst. Solids **61&62**, 571 (1984).
[33]P. J. Anthony and A. C. Anderson, Phys. Rev. B **14**, 5198 (1976); **16**, 3827 (1977).